This is an open access article published under an ACS AuthorChoice License, which permits copying and redistribution of the article or any adaptations for non-commercial purposes.

ACS OMEGA

Article

Cite This: ACS Omega 2019, 4, 20948−20954

http://pubs.acs.org/journal/acsodf

Synthesis of Polyacetylene-like Modified Graphene Oxide Aerogel and Its Enhanced Electrical Properties

Enrico Greco,[†,‡] Jing Shang,[*,†] Jiali Zhu,[†] and Tong Zhu[*,†,‡]

[†]State Key Joint Laboratory of Environmental Simulation and Pollution Control, College of Environmental Sciences and Engineering, and Center for Environment and Health and [‡]Beijing Innovation Center for Engineering Science and Advanced Technology (BIC-ESAT), Peking University, 5 Yiheyuan Road, Beijing 100871, P. R. China

ABSTRACT: A graphene-based or carbon-based aerogel is a three-dimensional (3D) solid material in which the carbon atoms are arranged in a sheet-like nanostructure. In this study, we report the synthesis of low-density polymer-modified aerogel monoliths by 3D macroassemblies of graphene oxide sheets that exhibit significant internal surface areas (982 m^2/g) and high electrical conductivity (~0.1 to 1 × 10^2 S/cm). Different types of materials were prepared to obtain a single monolithic solid starting from a suspension of single-layer graphene oxide (GO) sheets and a polymer, made from the precursors 4-carboxybenzaldehyde and poly(vinyl alcohol). These materials were used to cross-link the individual sheets by covalent bonds, resulting in wet-gels that were supercritically dried and then, in some cases, thermally reduced to yield graphene aerogel composites. The average densities were approaching 15−20 mg/cm^3. This approach allowed for the modulation of the distance between the sheets, pore dimension, surface area, and related properties. This specific GO/polymer ratio has suitable malleability, making it a viable conductive material for use in 3D printing; it also has other properties suitable for energy storage, catalysis, sensing and biosensing applications, bioelectronics, and superconductors.

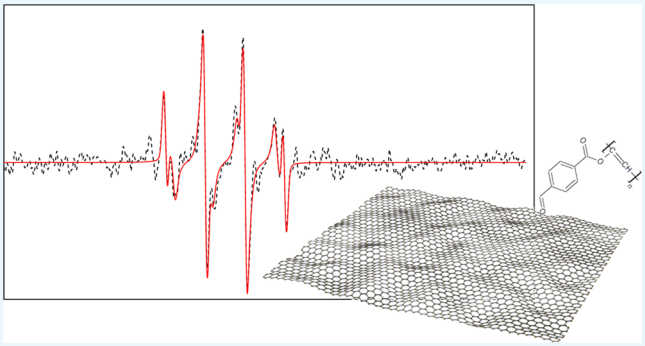

1. INTRODUCTION

Graphene and graphene oxide are one-atom-thick planar two-dimensional (2D) sheets of carbon atoms, sp^2-bonded, with a dense honeycomb-packed crystal lattice. The distinctive natural disposition of carbon atoms gives them a unique set of properties such as electronic, chemical, and mechanical.[1−4]

In the past few years, a significant number of researches have shown the potential applications of graphene-based sheets and their impact in a wide range of technologies including energy storage,[5−9] especially supercapacitors,[10,11] catalysis,[12−15] sensing,[9,12,16] and mechanically enhanced composites.[17−19] However, three-dimensional (3D) structures based on this extraordinary nanomaterial have not been well studied, and their synthesis or fabrication is limited to a few methods.[20−30]

Aerogels are 3D materials with open-cell foam structures, high relative surface areas, and nanoscale pores and cell sizes. One of the first developed and most commonly known aerogel is silica aerogel.[31−33] More recently, it has been demonstrated that graphene can be used as a building material for carbon-based aerogels composed of a network of different clustered carbon nanostructures.[34−36] Carbon-based aerogels show some similar properties to silica aerogels but with different mechanical behaviors and a capacity for electrical conductivity that depends heavily on their density.[37−40] Some interactions with light have also been reported. Specifically, carbon-based aerogels can absorb light in the visible and infrared spectra (they reflect only 0.3% of radiation between 250 nm and 14.3 μm).[41,42] The thermal conductivity of carbon aerogels tends to be equal to or less than air because these solids conduct heat only through thin chains of atoms, except in the case of some specific structural modifications.[43−46] It would be desirable to develop three-dimensional composite nanostructures with the extraordinary functionalities of graphene and other materials that modulate aerogel properties.

Previous reports focused on the high stability of graphene oxide (GO) suspensions to assemble an initial GO macrostructure, which was then thermally reduced to yield a 3D graphene network.[23,24] Others used a polymer to reinforce the structure[47] because the GO aerogel (GOA) structure is usually maintained by noncovalent cross-link-like van der Waals forces without any chemoelectric bonds.[48] This resulted in a relative surface area lower than that of the 2D-GO,[49] and the bulk electrical conductivities of these assemblies only reached approximately 5 × 10^{-1} S/cm[48,50] even in the case of metal doping.[50] This value is about 5 orders of magnitude lower than the conductivity reported for single graphene sheets.[50] Taken together, these and other results[51,52] underscore the importance of generating or determining the physical bonds between the GO sheets while maintaining the original properties, which would increase the potential utility of 3D graphene macroassemblies.

Received: July 8, 2019
Accepted: November 14, 2019
Published: December 2, 2019

Downloaded via 147.94.134.140 on October 20, 2020 at 16:32:08 (UTC).
See https://pubs.acs.org/sharingguidelines for options on how to legitimately share published articles.

© 2019 American Chemical Society

DOI: 10.1021/acsomega.9b02097
ACS Omega 2019, 4, 20948−20954

Table 1. List of Samples

sample name	GO susp. (mg/mL)		polymer/GO	notes
GOA0	25			graphene Oxide Aerogel control sample without polymer
GOA1	0.1	2:1	2:1	the polymer/GO ratio does not allow the formation of a proper structure. A wet-gel is formed, but the structure completely broke under SFE.
GOA2	0.5	2:1	1.5:1	the result after the SFE process is not a monolith; the sample has not strong structural integrity.
GOA3	5	2:1	1:1	
GOA4	10	2:1	1:1.5	
GOA5	25	2:1	1:3	
GOA6	25	2:1	1:10	
GOA7	0.1	2:1	5:1	the high polymer/GO ratio does not allow the formation of a proper structure. The polymer tends to agglomerate.

In our study, we present a new method to obtain low-density graphene aerogels with high electrical conductivity and large surface areas starting from GO, 4-carboxybenzaldehyde (4-CBA), and poly(vinyl alcohol) (PVA) to create an intrinsically conducting polymer (ICP) by dehydrogenation.[53,54] Also, to obtain a conductive polymer during the first synthesis phase, another critical aspect in fabricating these macroassemblies was the formation of covalently bonded junctions between the ICP and individual graphene oxide sheets to reinforce the structure and provide electrical conductive interconnections between the sheets. The method presented here utilizes a precursor obtained by 4-CBA and PVA, (poly(4-formylperoxibenzoyl)acetylene), to knit together graphene oxide sheets into a macroscopic 3D structure. With this approach, we are able to produce monolithic graphene oxide architectures with low densities (approaching 15−20 mg/cm^3) and electrical conductivities more than 2 orders of magnitude higher than those reported for other graphene aerogels.[50] Furthermore, the relative surface areas are lower but comparable to the areas reported for 2D graphene sheets.[49,50]

2. EXPERIMENTAL SECTION

2.1. Sample Preparation. The first two steps of our synthesis involved the preparation of the graphene oxide using the Hummers approach[55] to oxidize graphene flakes. The graphene oxide was then added to absolute ethanol (99.9%, Beijing Tongguang) to create a suspension. The solid content in the graphene oxide suspension may range from about 0.1 to about 25 mg/mL, as shown in Table 1. The suspensions were dispersed using a Shumei KQ-250DB ultrasonicator (frequency ∼ 40 kHz, sonic power ∼ 80 W). Six cycles of 15 min each of ultrasonication alternated with 15 min of stops were used to exfoliate the graphite oxide, and a sol−gel solution was finally obtained. It is crucial in this phase to reduce the time of each cycle and increase the number of cycles to avoid an increase of temperature of the solution and consequently a loss of functional groups on the surface of the single GO sheet. Any loss of oxygen on the GO surface could have negative effects on the formation of the covalent bonds with the polymer. Therefore, this phase is extremely important and must be executed with maximum precision and attention.

The synthesis can be schematized as reported in Figure 1. The oxygen indicated with * is then used to link this new molecule with the GO by the OH on the surface of the sheets.

The optimal conditions for GO dispersions were evaluated by a range of sonication cycles from 15 to 120 min.

The ICP precursor was prepared in a solution of ethanol and Millipore water ranging from 0:1 to 99.9:1 v/v ratio using 4-carboxybenzaldehyde 98%, Alfa Aesar (it is possible to choose

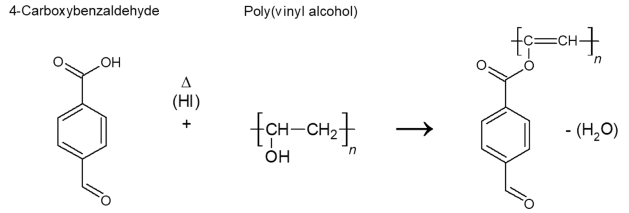

Figure 1. Step 1 of the reported synthesis of the polymer precursor and indication of the site (*) for the bonding with GO.

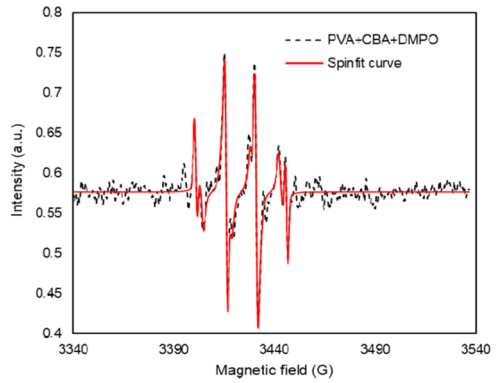

Figure 2. The primary and fitting EPR spectra of DMPO adducts.

similar molecules with one carboxylic functional group), and a long-chain polymer with at least two hydroxyl groups (such as poly(vinyl alcohol) >99% hydrolyzed, M_w 146 000−186 000 Da, Sigma-Aldrich). Hydroiodic acid (57 wt % in water) 0.1 wt % with respect to the PVA amount was used as a catalyst,[53] under stirring for 2 h. All of the samples presented in this work were prepared using 99.9:0.1 v/v EtOH/H_2O.

2.2. Characterization. Field-emission scanning electron microscopy (FE-SEM) was performed on an FE-SEM LEO Supra 55 VP along with a GEMINI column (Carl Zeiss, Germany) 5−10 keV (20 mA) in in-lens secondary electron imaging mode with a working distance of 2−8 mm, equipped with an Oxford Instrument Energy Dispersive Spectroscopy (EDX) analytical instrument.

Electron paramagnetic resonance (EPR) spectrometry (EMXnano, Bruker, Germany) was applied for the detection of radicals during and after the reaction. The parameters for EPR measurements were set with a modulation frequency of 100 kHz, a microwave frequency of 9.61 GHz, microwave power of 1.26 mW (19 dB), modulation amplitude of 2.0 G, a sweep width of 200 G, a time constant of 1.28 ms, and five scans. A nitrone spin trapping agent (5,5-dimethyl-1-pyrroline *N*-oxide ≥97%, DMPO, Sigma Aldrich) was used to form stable spin adducts with radicals.

DOI: 10.1021/acsomega.9b02097
ACS Omega 2019, 4, 20948−20954

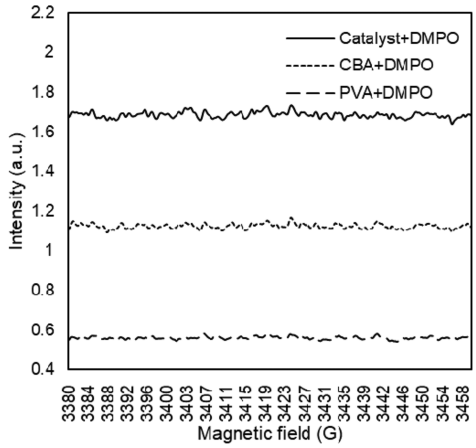

Figure 3. The EPR spectra of three control experiments.

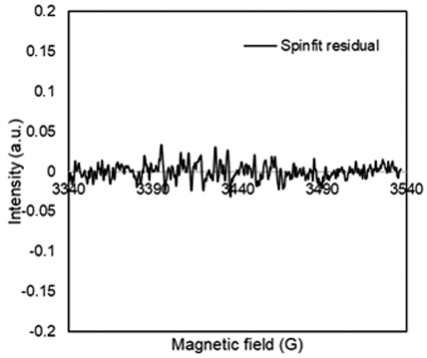

Figure 4. The residual of spinfit curve.

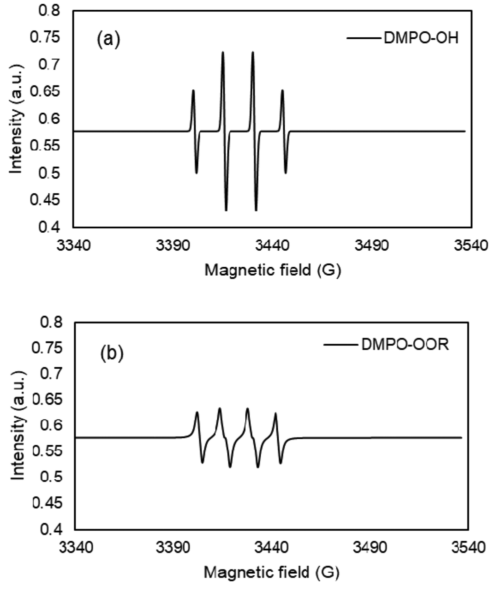

Figure 5. The separate EPR spectra for DMPO-OH (a) and DMPO-OOR (b) adducts in the mixed fitting curve.

Relative surface area and pore volume analyses were performed by Brunauer–Emmett–Teller (BET) and Barrett–Joyner–Halenda (BJH) methods by an ASAP 2000 Surface Area Analyzer (Micromeritics Instrument Corporation).

3. RESULTS AND DISCUSSION

Figure 2 shows the primary and the fitting EPR spectra of DMPO adducts. Spinfit results showed that in our reaction system, two kinds of radicals including hydroxyl and peroxyl radicals were formed, and the concentrations of hydroxyl and peroxyl radicals were 6.908×10^{11} and 2.300×10^{12} spins/mm^3, respectively. Control experiments showed that no radicals were formed (Figures 3–5), which confirmed that hydroxyl and peroxyl radicals were produced in our reaction system.

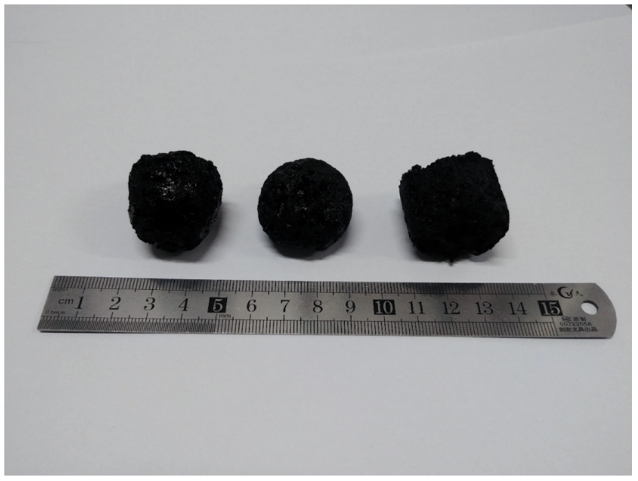

Figure 6. From the left: sample GOA4, GOA5, and GOA6 (Photograph by the authors).

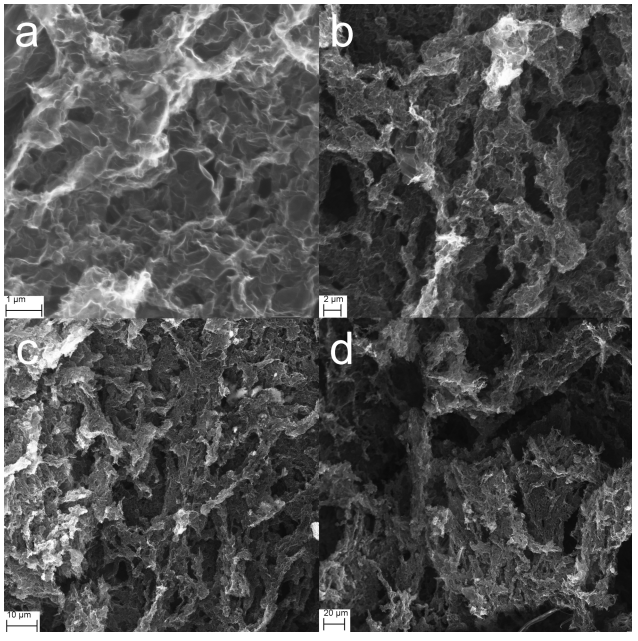

Figure 7. FE-SEM of the ICP-GO aerogels at different magnifications. It is possible to observe the porosity from a nanometer scale to micrometer. The images refer to GOA6 (a), GOA5 (b), GOA4 (c), and GOA3 (d).

The formation of the wet-gel was first activated by the addition of the polymer solution to the GO solution and a mechanical shock and was then transferred to a Teflon Becker, sealed and cured in a water bath at 87 °C for 5 h. Sodium carbonate (anhydrous, 0.1 wt % with respect to 4-CBA, Beijing Chemicals W.) was used as a catalyst. Polymer/GO wt ratio is typically in the range of about 0.1:1 to about 5:1. Depending on the application and the chemical/mechanical properties expected, other ratios could be suitable.

The resulted wet-gel was dried using an SFE-0.5 dryer using supercritical CO_2 at pressures of 7.5 to 8.0 ± 0.1 MPa and

DOI: 10.1021/acsomega.9b02097
ACS Omega 2019, 4, 20948−20954

Table 2. Relative Surface Areas and Pore Volumes

sample name	relative surface areas (BET) (m^2/g)	pore volumes (BJH) 10−50 nm (%)	pore volumes (BJH) 50−500 nm (%)	pore volumes (BJH) 500−1000 nm (%)
GOA0	1124.8	55.3	19.6	25.1
GOA3	557.4	44.1	32.4	23.5
GOA4	719.3	51.0	37.3	11.7
GOA5	788.7	48.2	31.6	20.2
GOA6	982.2	62.8	25.2	12.0

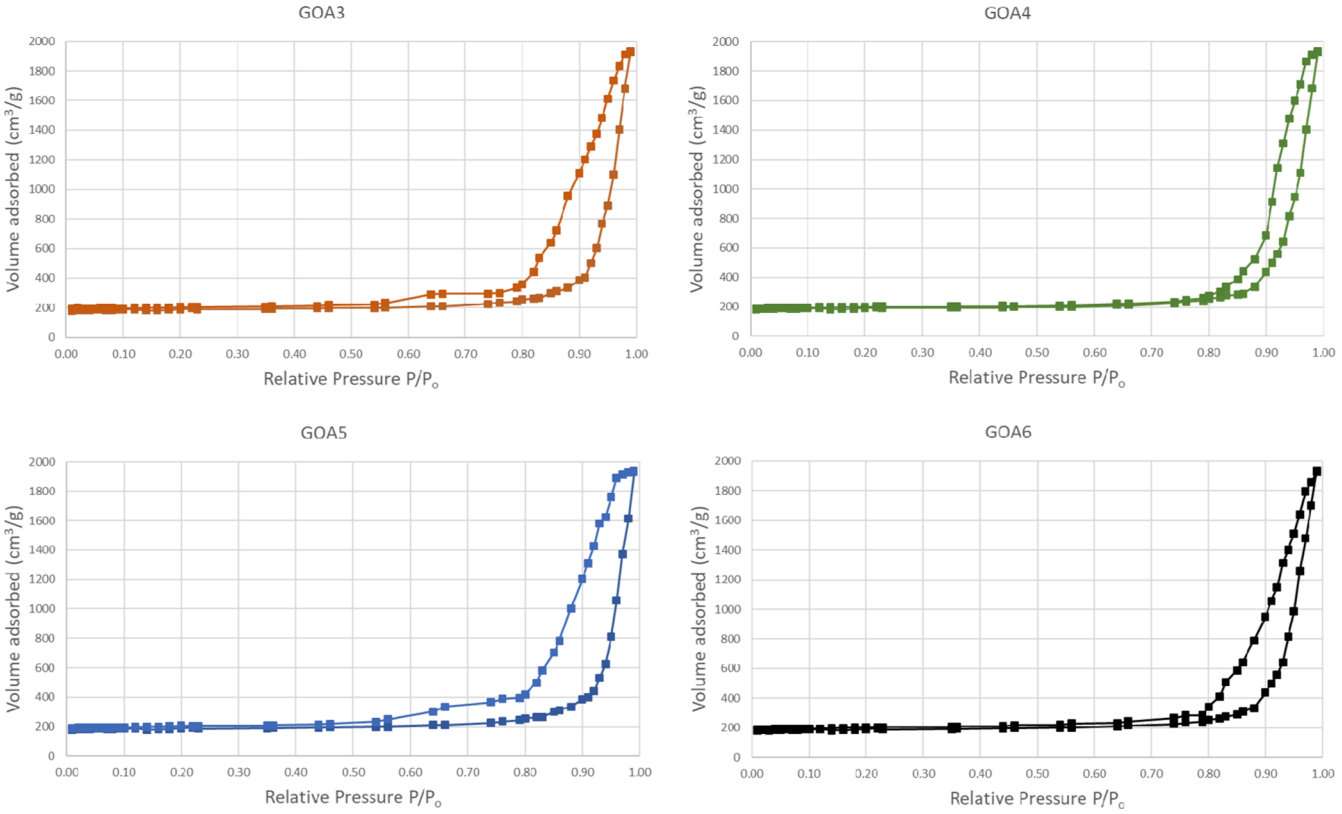

Figure 8. Nitrogen adsorption/desorption isotherm for the ICP-GO aerogels.

temperatures between 50.0 and 55.0 ± 0.5 °C. The system works with a flow rate of 1 L × h^{-1} using a separation chamber for the elimination of the extracted solvent and to obtain the samples shown in Figure 6. Some samples were pyrolyzed at 200 °C under N_2 atmosphere for 6 h to reduce all of the graphene oxide to graphene. Any thermal treatment of the aerogel should be conducted under conditions that avoid the decomposition of the polymer network. A typical range should be about 120 to 450 °C.

FE-SEM showed a random and densely oriented 3D network sheet-like structures of the graphene aerogel (Figure 7a,d) similar to those seen in previous reports.[35,56] The sizes of the sheets ranged from hundreds of nanometers to several micrometers. Using a higher magnification, the GO sheets network was thin enough to be transparent (Figure 7a).

We did not observe any agglomeration or nanoparticles of polymer on the graphene oxide sheets or other sites, although more than half of the weight in the aerogel was attributed to the polymer. When the ICP/GO wt % ratio was more than 1:1, the polymerization and the formation of the GOA did not occur. It is also clear that a synthesis where the junctions are mediated by carbonyl and carboxyl functional groups instead of hydroxyl groups prevents the formation of polymer random-coils.[57−61] In this case, the physical cross-links occur preferentially at the oxygen on the surface of the graphene oxide forming covalent bonds between individual sheets and the polymer formed a single macroassembly structure. The EDX analysis shows mainly carbon in all of the samples. Traces of iodine and calcium were found in sample GOA3.

Determination of the bulk densities was obtained from the physical dimensions and mass of each sample.

To measure the relative surface area and the pore volume, approximately 0.1 g of each sample was heated to 150 °C under vacuum (10^{-5} Torr) overnight (at least 12 h) to remove all adsorbed species. The list of results is reported in Table 2. The sample GOA1, GOA2, and GOA7 were not measured because of the reasons explained in the notes of Table 1.

The nitrogen adsorption/desorption isotherm for the ICP-GO aerogel (Figure 8) showed a type IV curve, indicating that the material is mesoporous. The type three hysteresis loop[62,63] occurred at high relative pressure and was associated with adsorption in the nanoporous structures, consistent with the aggregates observed using FE-SEM. The pore size distribution for the aerogel was determined by the BJH method,[62] which showed no clear distribution of the pore volume with three different macrogroups: one lay in the 10−50 nm range, most in

DOI: 10.1021/acsomega.9b02097
ACS Omega 2019, 4, 20948−20954

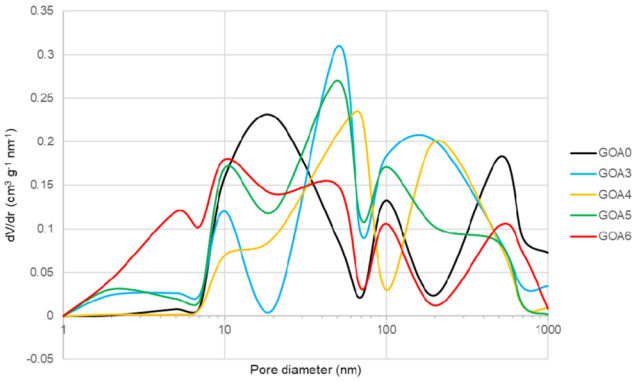

Figure 9. Pore size distribution of the samples GOA0, GOA3, GOA4, GOA5, and GOA6.

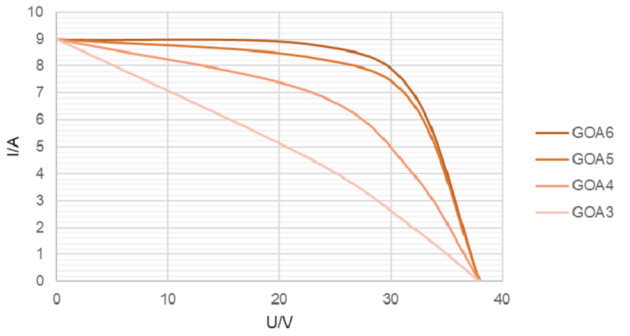

Figure 10. U-I curves of the samples GOA0, GOA3, GOA4, GOA5, and GOA6.

50−500 nm range, and a little in the 500−1000 nm range (Table 2 and Figures 8 and 9). The peak pore diameter was 126 nm. The BET surface area[64−66] for the aerogel strongly depended on the ratio between the polymer and GO during the synthesis, and the higher value was 982 m^2/g. The theoretical value of the surface area for a single graphene oxide sheet is about 2600 m^2/g,[50,67] but our samples showed lower values probably due to layering or overlapping of graphene oxide sheets within the assembly. Nevertheless, the measured surface area was higher than other values reported for high-quality GO aerogels prepared via hydrogen arc discharge,[49] or GO-RF,[35,43] and it was three times higher than that of the CNT aerogel.[68]

The four-probe method was used to measure the electrical conductivity with metal electrodes attached to the ends of cylindrical samples. Current (100 mA) was transmitted through the sample during the measurement, and the voltage drop was measured over distances of 6 to 7 mm. At least 10 measurements were taken on each sample, and results were averaged and reported in Table 2.

The bulk electrical conductivity (Table 3) of the polymer-modified graphene oxide aerogel was (sample GOA6) 128 S/cm,

Table 3. Electrical Conductivities Compared with Other Samples Reported Previously

sample name	electrical conductivity (S/cm)
GOA0	103.2
GOA3	12.3
GOA4	31.6
GOA5	54.2
GOA6	128.1
reference[69]	0.6 for non-reinforced 10^{-5} for reinforced
reference[70]	5.3
reference[71]	50
reference[72]	30
reference[73]	10^{-3}−10^{-1}

about 2−3 orders of magnitude higher than those reported for other 3D graphene materials prepared with other methods.[48,50] It is our opinion that this extraordinarily high conductivity and not the intuitively U-I behavior (Figure 10) is due to a rearrangement in the network morphology (many ripples in fixed positions) of the graphene oxide sheets in a 3D system. In congruence with the morphological differences, a substantial reduction in resistance at the connections between graphene sheets compared to those at the van der Waals bonds along with the use of an intrinsically conducting polymer could increase the mobility of the electrons and phonons. A more detailed discussion about the theoretical nature and the behavior of the charges in our polymer-modified aerogel will be presented in a forthcoming paper.

In conclusion, we prepared a macroscopic 3D polymer composite graphene oxide aerogel with large surface area and high electrical conductivity. Our approach used one molecule with a carboxyl and a carbonyl functional group to bind the hydroxyl group to a second molecule. It was used because of its long chain that could obtain conjugated bonds andto space out the graphene oxide sheets. We were able to modulate the density, the pore dimension, and the conductivity just by changing the polymer/GO ratio. Due to these properties, these 3D graphene assemblies have potential relevance in a large number of applications as conductive 3D printing, energy storage, electrocatalysis, sensors and biosensors, and electro-biointerfaces.

AUTHOR INFORMATION

Corresponding Authors

*E-mail: shangjing@pku.edu.cn (J.S.).
*E-mail: tzhu@pku.edu.cn (T.Z.).

ORCID

Enrico Greco: 0000-0003-1564-4661
Jing Shang: 0000-0002-9335-139X

Author Contributions

E.G. conceived the methods, prepared the materials, and made the characterizations, J.Z. made the EPR, J.S. and T.Z. conceived the idea, coordinated the work, and revised the manuscript.

Notes

The authors declare no competing financial interest.

ACKNOWLEDGMENTS

The authors are grateful to the financial support provided by the National Natural Science Foundation of China (Grant Nos. 21876003 and 21577003) and the National Key Research and Development Program of China (No. 2016YFC0202200). The authors declare no competing financial interests. The authors want to acknowledge Dr. Joseph Valentine for the revision of the text.

REFERENCES

(1) Castro Neto, A. H.; Guinea, F.; Peres, N. M. R.; Novoselov, K. S.; Geim, A. K. The Electronic Properties of Graphene. *Rev. Mod. Phys.* **2009**, *81*, 109−162.

(2) Ritter, K. A.; Lyding, J. W. The Influence of Edge Structure on the Electronic Properties of Graphene Quantum Dots and Nanoribbons. *Nat. Mater.* **2009**, *8*, 235.

DOI: 10.1021/acsomega.9b02097
ACS Omega 2019, 4, 20948−20954

(3) Mattevi, C.; Eda, G.; Agnoli, S.; Miller, S.; Mkhoyan, K. A.; Celik, O.; Mastrogiovanni, D.; Granozzi, G.; Garfunkel, E.; Chhowalla, M. Evolution of Electrical, Chemical, and Structural Properties of Transparent and Conducting Chemically Derived Graphene Thin Films. *Adv. Funct. Mater.* **2009**, *19*, 2577−2583.
(4) Rafiee, M. A.; Rafiee, J.; Wang, Z.; Song, H.; Yu, Z.-Z.; Koratkar, N. Enhanced Mechanical Properties of Nanocomposites at Low Graphene Content. *ACS Nano* **2009**, *3*, 3884−3890.
(5) Raccichini, R.; Varzi, A.; Passerini, S.; Scrosati, B. The Role of Graphene for Electrochemical Energy Storage. *Nat. Mater.* **2015**, *14*, 271−279.
(6) Pumera, M. Graphene-Based Nanomaterials for Energy Storage. *Energy Environ. Sci.* **2011**, *4*, 668−674.
(7) Liu, J.; Chen, J. S.; Wei, X.; Lou, X. W.; Liu, X. W. Sandwich-like, Stacked Ultrathin Titanate Nanosheets for Ultrafast Lithium Storage. *Adv. Mater.* **2011**, *23*, 998−1002.
(8) Wu, Z.-S.; Zhou, G.; Yin, L.-C.; Ren, W.; Li, F.; Cheng, H.-M. Graphene/Metal Oxide Composite Electrode Materials for Energy Storage. *Nano Energy* **2012**, *1*, 107−131.
(9) Pumera, M. Electrochemistry of Graphene: New Horizons for Sensing and Energy Storage. *Chem. Rec.* **2009**, *9*, 211−223.
(10) Stoller, M. D.; Park, S.; Zhu, Y.; An, J.; Ruoff, R. S. Graphene-Based Ultracapacitors. *Nano Lett.* **2008**, *8*, 3498−3502.
(11) El-Kady, M. F.; Kaner, R. B. Scalable Fabrication of High-Power Graphene Micro-Supercapacitors for Flexible and on-Chip Energy Storage. *Nat. Commun.* **2013**, *4*, No. 1475.
(12) Shen, J.; Zhu, Y.; Yang, X.; Li, C. Graphene Quantum Dots: Emergent Nanolights for Bioimaging, Sensors, Catalysis and Photovoltaic Devices. *Chem. Commun.* **2012**, *48*, 3686.
(13) Machado, B. F.; Serp, P. Graphene-Based Materials for Catalysis. *Catal. Sci. Technol.* **2012**, *2*, 54−75.
(14) Sun, S.; Zhang, G.; Gauquelin, N.; Chen, N.; Zhou, J.; Yang, S.; Chen, W.; Meng, X.; Geng, D.; Banis, M. N.; et al. Single-Atom Catalysis Using Pt/Graphene Achieved through Atomic Layer Deposition. *Sci. Rep.* **2013**, *3*, No. 1775.
(15) Kong, X.-K.; Chen, C.-L.; Chen, Q.-W. Doped Graphene for Metal-Free Catalysis. *Chem. Soc. Rev.* **2014**, *43*, 2841−2857.
(16) Di Mauro, A.; Randazzo, R.; Spanò, S. F.; Compagnini, G.; Gaeta, M.; D'Urso, L.; Paolesse, R.; Pomarico, G.; Di Natale, C.; Villari, V.; et al. Vortexes Tune the Chirality of Graphene Oxide and Its Non-Covalent Hosts. *Chem. Commun.* **2016**, *52*, 13094−13096.
(17) Fang, M.; Wang, K.; Lu, H.; Yang, Y.; Nutt, S. Covalent Polymer Functionalization of Graphene Nanosheets and Mechanical Properties of Composites. *J. Mater. Chem.* **2009**, *19*, 7098−7105.
(18) Baldino, L.; Sarno, M.; Cardea, S.; Irusta, S.; Ciambelli, P.; Santamaria, J.; Reverchon, E. Formation of Cellulose Acetate−Graphene Oxide Nanocomposites by Supercritical CO_2 Assisted Phase Inversion. *Ind. Eng. Chem. Res.* **2015**, *54*, 8147−8156.
(19) Innocenzi, P.; Malfatti, L.; Carboni, D. Graphene and Carbon Nanodots in Mesoporous Materials: An Interactive Platform for Functional Applications. *Nanoscale* **2015**, *7*, 12759−12772.
(20) Mi, X.; Huang, G.; Xie, W.; Wang, W.; Liu, Y.; Gao, J. Preparation of Graphene Oxide Aerogel and Its Adsorption for Cu 2+ Ions. *Carbon* **2012**, *50*, 4856−4864.
(21) Meng, F.; Zhang, X.; Xu, B.; Yue, S.; Guo, H.; Luo, Y. Alkali-Treated Graphene Oxide as a Solid Base Catalyst: Synthesis and Electrochemical Capacitance of Graphene/Carbon Composite Aerogels. *J. Mater. Chem.* **2011**, *21*, 18537−18539.
(22) Zhang, X.; Sui, Z.; Xu, B.; Yue, S.; Luo, Y.; Zhan, W.; Liu, B. Mechanically Strong and Highly Conductive Graphene Aerogel and Its Use as Electrodes for Electrochemical Power Sources. *J. Mater. Chem.* **2011**, *21*, 6494−6497.
(23) Worsley, M. A.; Pauzauskie, P. J.; Olson, T. Y.; Biener, J.; Satcher, J. H.; Baumann, T. F. Synthesis of Graphene Aerogel with High Electrical Conductivity. *J. Am. Chem. Soc.* **2010**, *132*, 14067−14069.
(24) Cheng, Y.; Zhou, S.; Hu, P.; Zhao, G.; Li, Y.; Zhang, X.; Han, W. Enhanced Mechanical, Thermal, and Electric Properties of Graphene Aerogels via Supercritical Ethanol Drying and High-Temperature Thermal Reduction. *Sci. Rep.* **2001**, *7*, No. 1439.
(25) Chen, W.; Li, S.; Chen, C.; Yan, L. Self-Assembly and Embedding of Nanoparticles by in Situ Reduced Graphene for Preparation of a 3D Graphene/Nanoparticle Aerogel. *Adv. Mater.* **2011**, *23*, 5679−5683.
(26) Tang, Z.; Shen, S.; Zhuang, J.; Wang, X. Noble-Metal-Promoted Three-Dimensional Macroassembly of Single-Layered Graphene Oxide. *Angew. Chem.* **2010**, *122*, 4707−4711.
(27) Vickery, J. L.; Patil, A. J.; Mann, S. Fabrication of Graphene-Polymer Nanocomposites With Higher-Order Three-Dimensional Architectures. *Adv. Mater.* **2009**, *21*, 2180−2184.
(28) Liu, F.; Seo, T. S. A Controllable Self-Assembly Method for Large-Scale Synthesis of Graphene Sponges and Free-Standing Graphene Films. *Adv. Funct. Mater.* **2010**, *20*, 1930−1936.
(29) Xu, Y.; Sheng, K.; Li, C.; Shi, G. Self-Assembled Graphene Hydrogel via a One-Step Hydrothermal Process. *ACS Nano* **2010**, *4*, 4324−4330.
(30) Zu, S.-Z.; Han, B.-H. Aqueous Dispersion of Graphene Sheets Stabilized by Pluronic Copolymers: Formation of Supramolecular Hydrogel. *J. Phys. Chem. C* **2009**, *113*, 13651−13657.
(31) Soleimani Dorcheh, A.; Abbasi, M. H. Silica Aerogel; Synthesis, Properties and Characterization. *J. Mater. Process. Technol.* **2008**, *199*, 10−26.
(32) Schaefer, D. W.; Keefer, K. D. Structure of Random Porous Materials: Silica Aerogel. *Phys. Rev. Lett.* **1986**, *56*, 2199−2202.
(33) Gurav, J. L.; Jung, I.-K.; Park, H.-H.; Kang, E. S.; Nadargi, D. Y. Silica Aerogel: Synthesis and Applications. *J. Nanomater.* **2010**, *2010*, 1−11.
(34) Lin, Z.; Wang, X. Nanostructure Engineering and Doping of Conjugated Carbon Nitride Semiconductors for Hydrogen Photosynthesis. *Angew. Chem.* **2013**, *125*, 1779−1782.
(35) Worsley, M. A.; Kucheyev, S. O.; Satcher, J. H.; Hamza, A. V.; Baumann, T. F. Mechanically Robust and Electrically Conductive Carbon Nanotube Foams. *Appl. Phys. Lett.* **2009**, *94*, No. 073115.
(36) Lalia, B. S.; Ahmed, F. E.; Shah, T.; Hilal, N.; Hashaikeh, R. Electrically Conductive Membranes Based on Carbon Nanostructures for Self-Cleaning of Biofouling. *Desalination* **2015**, *360*, 8−12.
(37) Sarno, M.; Baldino, L.; Scudieri, C.; Cardea, S.; Ciambelli, P.; Reverchon, E. Supercritical CO2 Processing to Improve the Electrochemical Properties of Graphene Oxide. *J. Supercrit. Fluids* **2016**, *118*, 119−127.
(38) Zhang, X.; Sui, Z.; Xu, B.; Yue, S.; Luo, Y.; Zhan, W.; Liu, B. Mechanically Strong and Highly Conductive Graphene Aerogel and Its Use as Electrodes for Electrochemical Power Sources. *J. Mater. Chem.* **2011**, *21*, 6494.
(39) Sun, H.; Xu, Z.; Gao, C. Multifunctional, Ultra-Flyweight, Synergistically Assembled Carbon Aerogels. *Adv. Mater.* **2013**, *25*, 2554−2560.
(40) Zhu, C.; Han, T. Y.-J.; Duoss, E. B.; Golobic, A. M.; Kuntz, J. D.; Spadaccini, C. M.; Worsley, M. A. Highly Compressible 3D Periodic Graphene Aerogel Microlattices. *Nat. Commun.* **2015**, *6*, No. 6962.
(41) Wang, J.; Ellsworth, W. Graphene and Graphene Oxide Aerogels. US Patent 8,871,821 B2, 2008.
(42) Dabidian, N.; Kholmanov, I.; Khanikaev, A. B.; Tatar, K.; Trendafilov, S.; Mousavi, S. H.; Magnuson, C.; Ruoff, R. S.; Shvets, G. Electrical Switching of Infrared Light Using Graphene Integration with Plasmonic Fano Resonant Metasurfaces. *ACS Photonics* **2015**, *2*, 216−227.
(43) Al-Muhtaseb, S. A.; Ritter, J. A. Preparation and Properties of Resorcinol-Formaldehyde Organic and Carbon Gels. *Adv. Mater.* **2003**, *15*, 101−114.
(44) Hrubesh, L. W.; Pekala, R. W. Thermal Properties of Organic and Inorganic Aerogels. *J. Mater. Res.* **1994**, *9*, 731−738.
(45) Lu, X.; Caps, R.; Fricke, J.; Alviso, C. T.; Pekala, R. W. Correlation between Structure and Thermal Conductivity of Organic Aerogels. *J. Non-Cryst. Solids* **1995**, *188*, 226−234.
(46) Lu, X.; Nilsson, O.; Fricke, J.; Pekala, R. W. Thermal and Electrical Conductivity of Monolithic Carbon Aerogels. *J. Appl. Phys.* **1993**, *73*, 581−584.
(47) Bai, H.; Li, C.; Wang, X.; Shi, G. A PH-Sensitive Graphene Oxide Composite Hydrogel. *Chem. Commun.* **2010**, *46*, 2376−2378.

DOI: 10.1021/acsomega.9b02097
ACS Omega 2019, 4, 20948−20954

(48) Liu, F.; Wang, C.; Tang, Q. Conductivity Maximum in 3D Graphene Foams. *Small* **2018**, *14*, No. 1801458.
(49) Wu, Z. S.; Ren, W.; Gao, L.; Zhao, J.; Chen, Z.; Liu, B.; Tang, D.; Yu, B.; Jiang, C.; Cheng, H. M. Synthesis of Graphene Sheets with High Electrical Conductivity and Good Thermal Stability by Hydrogen Arc Discharge Exfoliation. *ACS Nano* **2009**, *3*, 411−417.
(50) Nardecchia, S.; Carriazo, D.; Ferrer, M. L.; Gutiérrez, M. C.; Del Monte, F. Three Dimensional Macroporous Architectures and Aerogels Built of Carbon Nanotubes and/or Graphene: Synthesis and Applications. *Chem. Soc. Rev.* **2013**, *42*, 794−830.
(51) Guan, L.-Z.; Zhao, L.; Wan, Y.-J.; Tang, L.-C. Three-Dimensional Graphene-Based Polymer Nanocomposites: Preparation, Properties and Applications. *Nanoscale* **2018**, *10*, 14788−14811.
(52) Cong, H.-P.; Chen, J.-F.; Yu, S.-H. Graphene-Based Macroscopic Assemblies and Architectures: An Emerging Material System. *Chem. Soc. Rev.* **2014**, *43*, 7295−7325.
(53) Sreeram, A.; Krishnan, S.; DeLuca, S. J.; Abidnejad, A.; Turk, M. C.; Roy, D.; Honarvarfard, E.; Goulet, P. J. G. Simultaneous Electronic and Ionic Conduction in Ionic Liquid Imbibed Polyacetylene-like Conjugated Polymer Films. *RSC Adv.* **2015**, *5*, 88425−88435.
(54) Menegazzo, F.; Fantinel, T.; Signoretto, M.; Pinna, F. Metal Dispersion and Distribution in Pd-Based PTA Catalysts. *Catal. Commun.* **2007**, *8*, 876−879.
(55) Hummers, W. S.; Offeman, R. E. Preparation of Graphitic Oxide. *J. Am. Chem. Soc.* **1958**, *80*, 1339.
(56) Yoo, E.; Kim, J.; Hosono, E.; Zhou, H.; Kudo, T.; Honma, I. Large Reversible Li Storage of Graphene Nanosheet Families for Use in Rechargeable Lithium Ion Batteries. *Nano Lett.* **2008**, *8*, 2277−2282.
(57) Vollmert, B. *Polymer Chemistry*; Springer Berlin Heidelberg, 1973.
(58) Mes, T.; van der Weegen, R.; Palmans, A. R. A.; Meijer, E. W. Single-Chain Polymeric Nanoparticles by Stepwise Folding. *Angew. Chem., Int. Ed.* **2011**, *50*, 5085−5089.
(59) Agarwal, U. S. Effect of Initial Conformation, Flow Strength, and Hydrodynamic Interaction on Polymer Molecules in Extensional Flows. *J. Chem. Phys.* **2000**, *113*, 3397−3403.
(60) Zhang, W.; Jin, W.; Fukushima, T.; Saeki, A.; Seki, S.; Aida, T. Supramolecular Linear Heterojunction Composed of Graphite-Like Semiconducting Nanotubular Segments. *Science* **2011**, *334*, 340−343.
(61) O'Connell, M. J.; Boul, P.; Ericson, L. M.; Huffman, C.; Wang, Y.; Haroz, E.; Kuper, C.; Tour, J.; Ausman, K. D.; Smalley, R. E. Reversible Water-Solubilization of Single-Walled Carbon Nanotubes by Polymer Wrapping. *Chem. Phys. Lett.* **2001**, *342*, 265−271.
(62) Barrett, E. P.; Joyner, L. G.; Halenda, P. P. The Determination of Pore Volume and Area Distributions in Porous Substances. I. Computations from Nitrogen Isotherms. *J. Am. Chem. Soc.* **1951**, *73*, 373−380.
(63) Lowell, S.; Shields, J. E.; Thomas, M. A.; Thommes, M. Characterization of Porous Solids and Powders: Surface Area, Pore Size and Density. *Characterization of Porous Solids III*; 2004; 129−139.
(64) Gelb, L. D.; Gubbins, K. E. Characterization of Porous Glasses: Simulation Models, Adsorption Isotherms, and the Brunauer-Emmett-Teller Analysis Method. *Langmuir* **1998**, *14*, 2097−2111.
(65) Pickett, G. Modification of the Brunauer Emmett Teller Theory of Multimolecular Adsorption. *J. Am. Chem. Soc.* **1945**, *67*, 1958−1962.
(66) Brunauer, S.; Emmett, P. H.; Teller, E. Adsorption of Gases in Multimolecular Layers. *J. Am. Chem. Soc.* **1938**, *60*, 309−319.
(67) Peigney, A.; Laurent, C.; Flahaut, E.; Bacsa, R. R.; Rousset, A. Specific Surface Area of Carbon Nanotubes and Bundles of Carbon Nanotubes. *Carbon* **2001**, *39*, 507−514.
(68) Worsley, M. A.; Pauzauskie, P. J.; Kucheyev, S. O.; Zaug, J. M.; Hamza, A. V.; Satcher, J. H.; Baumann, T. F. Properties of Single-Walled Carbon Nanotube-Based Aerogels as a Function of Nanotube Loading. *Acta Mater.* **2009**, *57*, 5131−5136.
(69) Bryning, M. B.; Milkie, D. E.; Islam, M. F.; Hough, L. A.; Kikkawa, J. M.; Yodh, A. G. Carbon Nanotube Aerogels. *Adv. Mater.* **2007**, *19*, 661−664.
(70) Meng, F.; Zhang, X.; Xu, B.; Yue, S.; Guo, H.; Luo, Y. Alkali-Treated Graphene Oxide as a Solid Base Catalyst: Synthesis and Electrochemical Capacitance of Graphene/Carbon Composite Aerogels. *J. Mater. Chem.* **2011**, *21*, 18537.
(71) Xie, X.; Hu, L.; Pasta, M.; Wells, G. F.; Kong, D.; Criddle, C. S.; Cui, Y. Three-Dimensional Carbon Nanotube−Textile Anode for High-Performance Microbial Fuel Cells. *Nano Lett.* **2011**, *11*, 291−296.
(72) Zhao, Y.; Liu, J.; Hu, Y.; Cheng, H.; Hu, C.; Jiang, C.; Jiang, L.; Cao, A.; Qu, L. Highly Compression-Tolerant Supercapacitor Based on Polypyrrole-Mediated Graphene Foam Electrodes. *Adv. Mater.* **2013**, *25*, 591−595.
(73) Guan, L. Z.; Gao, J. F.; Pei, Y. B.; Zhao, L.; Gong, L. X.; Wan, Y. J.; Zhou, H.; Zheng, N.; Du, X. S.; Wu, L. bin.; et al. Silane Bonded Graphene Aerogels with Tunable Functionality and Reversible Compressibility. *Carbon* **2016**, *107*, 573−582.

DOI: 10.1021/acsomega.9b02097
ACS Omega 2019, 4, 20948−20954